Observation of Precursor Magnetic Oscillations to the *H*-Mode Transition of the ASDEX Tokamak

K. Toi,[a] J. Gernhardt, O. Klüber, and M. Kornherr
Max-Planck-Institut für Plasmaphysik, EURATOM-Association, D-8046 Garching, München, Federal Republic of Germany
(Received 4 April 1988)

A precursor to the *L*-to-*H* transition is identified in magnetic fluctuations of the ASDEX *H*-mode discharges which are initiated without a sawtooth oscillation. This precursor is the $m=4$, $n=1$ mode which is uncoupled with the $m=1$, $n=1$ internal mode. This precursor appears also near the edge localized mode and *H*-to-*L* transition. The behavior in time of the amplitude suggests that these transitions are governed not by the edge electron temperature, but by the edge current density.

PACS numbers: 52.55.Fa, 52.35.Py, 52.50.Gj

Since the improved-confinement regime, "*H* mode," was discovered in the poloidal divertor tokamak ASDEX,[1] it has been achieved in divertor[2-5] and limiter[5] configurations. In the *H*-mode discharge, the electron temperature and density at the plasma edge (T_{eb},n_{eb}) rise significantly *just after* the *L*-to-*H* transition (*H*-mode transition), but there is also a continuous rise in T_{eb} prior to the transition in many cases when there is a delayed transition. The *H*-mode transition is often initiated by a sudden rise in T_{eb} due to a sawtooth crash, which is interpreted to mean that T_{eb} reaches a certain threshold for the transition.[6] The initiation by a sawtooth mostly occurs at low heating power and high plasma current.[7] In discharges with high heating power in ASDEX, however, the transition is often initiated without a sawtooth. *H*-mode discharges initiated without a sawtooth in the Poloidal Divertor Experiment (PDX) tokamak[8] showed that there was no simple threshold for the transition in T_{eb}. As an alternative to the requirement of sufficiently high T_{eb}, the *H* mode could be triggered by the formation of finite current density at the edge ($j_{\varphi b}$).

In this Letter, we try to analyze this aspect for the *H*-mode discharges in ASDEX, with the help of MHD modes detected by Mirnov probes because these modes may successfully indicate the change in the current-density (j_φ) profile. This work was motivated by two types of recent theories which discuss the role of a current-density profile in the *H*-mode transition: (i) One[9-11] derives the current-density profile with finite $j_{\varphi b}$ relevant to the *H* mode from an energy principle and predicts the substantial improvement of the confinement with such a j_φ profile, and (ii) the other[12] predicts the stabilization of the ideal ballooning mode due to finite $j_{\varphi b}$ in a divertor plasma. Note that it is difficult to see unambiguously whether T_{eb} or $j_{\varphi b}$ is the leading factor for the transition, because of the strong coupling of the current density to the electron temperature via the electrical conductivity in a tokamak. Accordingly, we concentrate our attention on the *H*-mode discharge which is characterized by no obvious rise in T_{eb} prior to the transition. In such a discharge, we have found coherent magnetic oscillations which suggest the evolution of the j_φ profile from the peaked *L* type to the *H* type with finite $J_{\varphi b}$ prior to the *H*-mode transition.

In ASDEX, magnetic fluctuations ($\lesssim 100$ kHz) are detected by Mirnov probes installed in a vacuum chamber. Ten probes cover the poloidal circumference, with three positioned over 44° on the inside and with seven positioned over 102° on the outside of the torus, symmetric about the midplane.[13,14] Four probes are placed

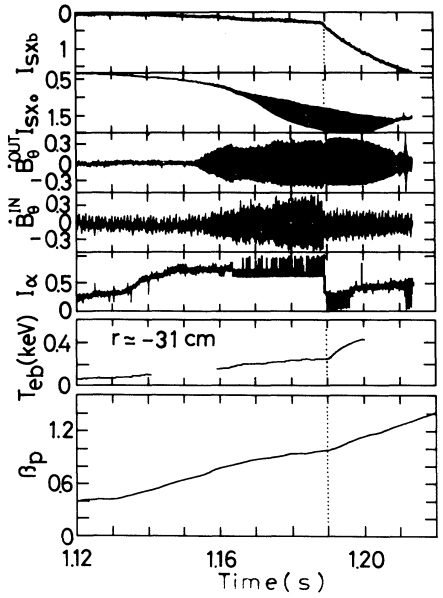

FIG. 1. Time evolution of soft-x-ray emissions at the plasma edge E_{sxb} ($r/r_s \simeq 0.95$) and center I_{sx0} ($r/r_s \simeq 0$), poloidal magnetic fluctuations $\dot{B}_\theta$ outside ($\theta = 180°$) and inside ($\theta = -22°$) the torus, H_α/D_α emission in the divertor chamber (I_α), edge electron temperature derived from the electron cyclotron emission T_{eb} ($r = R - R_0 \simeq -31$ cm) (the interruption is instrumental), and β_p obtained from a diamagnetic loop. $\dot{B}_\theta$ at $\theta = -22°$ is contaminated by rectifier noise ($f \simeq 1$ kHz). All data except T_{eb} are obtained in shot 18046. T_{eb} is measured in the neighboring shot (18053) with identical discharge conditions.

in the midplane outside the torus distributed over a toroidal angle of 156°. The signals ($\dot{B}_\theta$) are acquired by fast analog-to-digital converters with a 250-kHz sampling rate. H_α/D_α emission in a divertor chamber is also monitored by the fast analog-to-digital converter to define the time of the H-mode transition more accurately.

Figure 1 shows time behavior of the H-mode discharge initiated without a sawtooth in a double null divertor configuration. In this discharge, an H^0 beam of power 3.45 MW is coinjected into a deuterium plasma of electron density $\bar{n}_e \simeq 3\times10^{13}$ cm^{-3} at a cylindrical safety factor $q_a \simeq 3.3$ ($I_p = 320$ kA, $B_t = 2.2$ T, and separatrix radius $r_s \simeq 40$ cm). The H-mode transition occurs at $t \simeq 1.19$ s, exhibiting a sharp depression of H_α/D_α emission (I_α), a rapid rise in soft-x-ray emission at the plasma edge (I_{sxb}), and a further rise in poloidal β (β_p). Fluctuations of $\dot{B}_\theta$ and the central soft-x-ray emission (I_{sx0}) begin to rise about 35 ms before the transition. The raw (unfiltered) signal $\dot{B}_\theta$ inside the torus decreases obviously at the transition, while the outside one exhibits a slight dip then. As shown in Fig. 1, T_{eb} at $r \simeq -31$ cm rises gradually until 8 ms prior to the transition, and then stays constant ($\sim$240 eV) until the transition. It does not seem that the transition is triggered by high T_{eb} beyond the threshold, because T_{eb} stays constant for a long time (8 ms) prior to the transition, compared with the transition time which may be defined by the time of depression in I_α (in this case it is $\lesssim$0.1 ms).

In order to investigate the fine structure of the fluctuations observed in $\dot{B}_\theta$ and I_{sx0}, frequency spectra are calculated for 1024 data points for about 4.1 ms. Figure 2 shows the frequency spectra of $\dot{B}_\theta$ inside the torus and I_{sx0} just before and after the H-mode transition in Fig. 1. A peak at frequency $f = f_0$ in the spectrum of I_{sx0} corresponds to the $m=1$, $n=1$ internal mode, and the other peaks at $f = 2f_0$ and $3f_0$ to the higher harmonics such as $m=2$, $n=2$. These modes are localized near the $q=1$ surface. In the spectrum of $\dot{B}_\theta$, characteristic peaks are found at the same frequency ($f = f_0$, $2f_0$, and $3f_0$) as that of the internal mode. The most interesting oscillation peak is that at $f = f_*$, which is clearly found only in the spectrum of $\dot{B}_\theta$ during the L phase [Fig. 2(b)]. Only the intensity of this peak is reduced in the H phase.

We extract each characteristic frequency component from observed fluctuations by using an ideal filter method which is based on the fast Fourier transform. The essential procedure of this method is as follows: (1) Calculate a frequency spectrum by fast Fourier transform; (2) separate the spectrum into low-frequency (LF, $0 \leqq f \leqq f_L$), intermediate-frequency (IF, $f_L \leqq f \leqq f_H$), and high-frequency (HF, $f_H \leqq f$) components by lower and higher cutoff frequencies (f_L,f_H); (3) make the spectral power in the frequency range to be filtered to be zero; (4) retransform the filtered frequency spectrum into time series data. By analyzing test data composed of three frequency components, the relative deviations of amplitude and phase are estimated to be less than 1% for each filtered component. This method makes it possible to identify the mode numbers m and n of each frequency component successfully. For the discharge shown in Fig. 1 the HF component of $\dot{B}_\theta$ with $f \simeq f_0$ is identified as the $m=2$, $n=1$ mode. The higher-frequency component with $f \simeq 2f_0$ is the $m=3$, $n=2$ mode. The $m=2$, $n=1$ and $m=3$, $n=2$ modes propagate in the same direction with coinjected neutral beams. This $m=2$, $n=1$ (or $m=3$, $n=2$) mode is considered to be the mode driven by the $m=1$, $n=1$ (or $m=2$, $n=2$) internal mode through the toroidal and nonlinear couplings. Note that

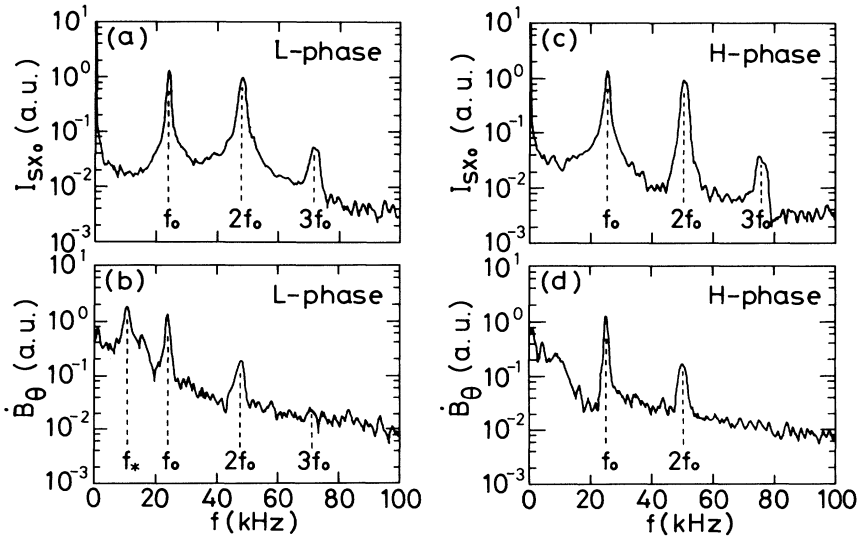

FIG. 2. Frequency spectra of I_{sx0} and $\dot{B}_\theta$ inside the torus. The spectra are calculated for just before (1.1850–1.1891 s) and after (1.1900–1.1941 s) the H-mode transition.

the driven mode is localized near a $q=1$ surface, in contrast to the linearly unstable $m=2$, $n=1$ or $m=3$, $n=2$ tearing mode.[15] On the other hand, the IF component with $f \simeq f_*$ is the $m=4$, $n=1$ mode propagating in the direction opposite to the neutral beams, and is uncoupled with the above-mentioned internal modes. This mode will be localized very close to the separatrix, since a resonant surface of $q=4$ is located there. While f_0 continuously increases from 11 to 25 kHz during the preceding L phase, f_* remains almost constant (8–10 kHz) and is comparable to the estimated electron diamagnetic drift frequency.

In Fig. 3, we give an enlargement of the transition phase shown in Fig. 1 together with the HF and IF components of $\dot{B}_\theta$ inside the torus. We obviously see the time sequence of events related to the H-mode transition. First, the amplitude of the $m=4$, $n=1$ IF component begins to decrease, and then the rise in I_{sxb} follows. Finally, the H_α/D_α emission I_α is depressed suddenly. The time lag of the depression from the beginning of the decrease in the IF-component amplitude is about 1 ms. The amplitude of the $m=2$, $n=1$ HF component decreases only gradually across the transition. The maximum fluctuation level $\tilde{B}_\theta/B_\theta$ at the probe position is $\sim 0.1\%$ for the $m=2$, $n=1$ mode and $\sim 0.2\%$ for the $m=4$, $n=1$ mode just prior to the transition. Note that the HF and IF components of $\dot{B}_\theta$ outside the torus also evolve similarly to those shown in Fig. 3, except for the amplitude.

The IF component suppressed just prior to the H-mode transition is again destabilized just prior to the H-to-L transition that is recognized by a sudden rise in the H_α/D_α emission (L-mode transition), having the same mode structure ($m=4$, $n=1$) and rotation direction. As shown in Fig. 4, I_α is suddenly enhanced ~ 0.2 ms after the excitation of the IF component, which is excited ~ 0.5 ms after a sudden decrease in I_{sxb}. Note that this L-mode transition occurs even at sufficiently high T_{eb} ($\simeq 580$ eV). It is thought that T_{eb} does not play a crucial role in this transition. The time behavior of I_α, I_{sxb}, and $\dot{B}_\theta$ near the edge localized mode[7] is very similar to that shown in Fig. 4, except that the recovery to the H phase occurs.

We discuss what type of instability is responsible for the above-mentioned IF component, which is characterized by a coherent nature and low mode number ($m=4$ and $n=1$). Both the microtearing mode driven by ∇T_e (Ref. 16) and the high-n ballooning mode driven by the global pressure gradient or the high β_p in the resistive plasma[17] are excluded because of these characteristics of the IF component. Moreover, the evidence that the character of the IF component remains unchanged in the range $\beta_p \simeq 0.7$–1.6 also supports this conclusion for the latter mode. There may be the possibility of a low-n ballooning mode driven by a local pressure gradient in the central low-shear region.[18] This possibility is also excluded by the relation among the observed modes of f_0, $2f_0$, and f_* with respect to the frequency, mode number, and rotation direction. A tearing or kink mode driven by ∇j_φ seems to be the most probable candidate for the IF component. However, no theoretical stability analysis of the mode in a realistic divertor configuration has been reported so far, except for an analysis on a simplified model.[19] The divertor plasma appears to have two basically different MHD-stable j_φ-profile options[20]: peaked L-type and H-type "pedestal" profiles. When the j_φ

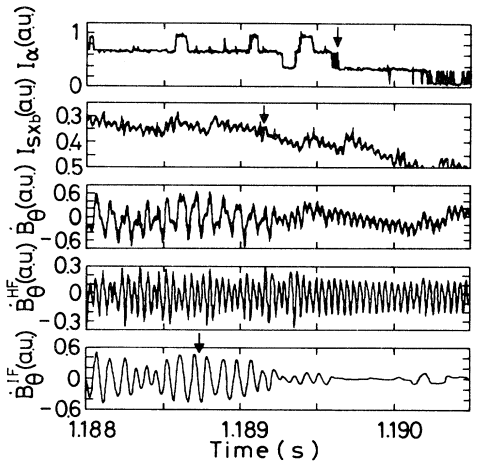

FIG. 3. Time evolution of I_α, I_{sxb}, unfiltered $\dot{B}_\theta$ inside the torus, $m=2$, $n=1$ HF component ($f \gtrsim 16$ kHz), and $m=4$, $n=1$ IF component ($4 \lesssim f \lesssim 16$ kHz) of the $\dot{B}_\theta$ near the H-mode transition. The arrows indicate the time when an obvious change of each signal occurs.

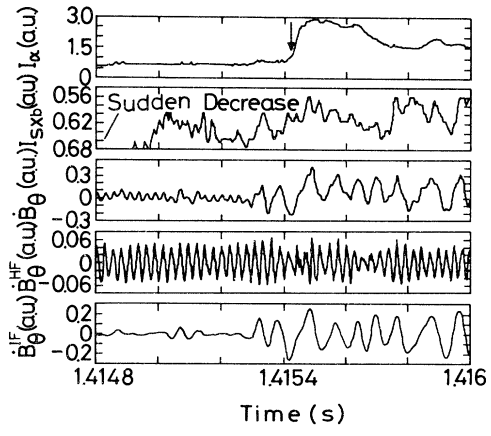

FIG. 4. Time evolution of typical plasma parameters near the L-mode transition (shot 18059), where the frequency band for HF and IF components is $f \gtrsim 31$ kHz and $4 \lesssim f \lesssim 31$ kHz, respectively. I_{sxb} suddenly decreases from ~ 1.0 at $t=1.4148$ s to ~ 0.6 for ~ 0.2 ms. The arrow indicates the L-mode transition.

profile evolves from the L-type to H-type or H-type to L-type profile near the transition, tearing or kink modes such as $m=2$, $n=1$; $m=3$, $n=1$; and $m=4$, $n=1$ may be destabilized or stabilized, depending on $j_{\varphi b}$ or ∇j_φ near the edge formed in the course of the profile evolution.[21] It is thought that the observed IF component merely indicates the change in the j_φ profile, and the j_φ profile instead of the component itself plays the important role in the transition, because the reduction rate of the time-integrated IF component across the H-mode transition is too significant to explain the degree of confinement improvement (Figs. 2 and 3). The same type of IF component is detected in discharges at $q_a \sim 2.6$ as well as $q_a \sim 3.3$ as presented here. However, the component is not always clearly distinguished near the H- or L-mode transition in H-mode discharges obtained under various conditions. It is conjectured that the mode characteristics of the IF component depend sensitively on the detailed shape of the j_φ profile near the edge.[21] Note that noninductive current driven by ∇_p and injected beams may also modify the j_φ profile appreciably near the H- and L-mode transitions. The above discussion on the j_φ profile in H-mode discharges seems to fit the above theory (i).[9-11] The other theory[12] (ii) may not be applicable because the pressure gradient at the edge just prior to the edge localized mode appears to be limited by the stability limit against the ballooning mode.[22]

As discussed in this Letter, the $m=4$, $n=1$ coherent magnetic oscillations observed near the H- and L-mode transitions are interpreted to be a tearing or kink mode driven by $j_{\varphi b}$ or ∇j_φ at the edge. The behavior of the oscillations suggests that the current-density profile plays an important role in both transitions, while the role of T_{eb} is not entirely excluded at present. We plan to study how the j_φ profile affects the stability of the ∇p- or ∇T_e-driven modes.

The authors acknowledge fruitful discussions with members of the ASDEX and NI teams. One of us (K.T.) would like to thank Dr. K. Grassie, Dr. O. Gruber, Dr. F. Wagner, and Dr. K. Lackner for stimulating discussions. He also is grateful to Dr. D. Eckhartt and Dr. F. Leuterer for continuing encouragement and hospitality. The authors also appreciate the help of Dr. C. K. Birdsall.

[a]Permanent address: Institute of Plasma Physics, Nagoya University, Nagoya 464, Japan.

[1]F. Wagner *et al.*, Phys. Rev. Lett. **49**, 1408 (1982).

[2]S. Kaye *et al.*, J. Nucl. Mater. **121**, 115 (1984).

[3]J. Luxon *et al.*, in *Proceeding of the Eleventh International Conference On Plasma Physics and Controlled Nuclear Fusion Research, Kyoto, Japan, 1986* (IAEA, Vienna, 1987), Vol. 1, p. 159.

[4]A. Tanga *et al.*, in Ref. 3, p. 65.

[5]K. Odajima *et al.*, in Ref. 3, p. 151.

[6]F. Wagner *et al.*, J. Nucl. Mater. **121**, 103 (1984).

[7]M. Keilhacker *et al.*, Plasma Phys. Controlled Fusion **26**, 49 (1984).

[8]R. Fonck *et al.*, in *Proceedings of the Fourth International Symposium on Heating of Toroidal Plasmas, Rome, 1984,* edited by H. Knoepfel and E. Sindoni (International School of Plasma Physics, Varenna, 1984), p. 37.

[9]D. Biskamp, Comments Plasma Phys. Controlled Fusion **10**, 165 (1986).

[10]B. B. Kadomtsev, presented at IAEA Specialists Meeting on Confinement in Tokamaks with Intense Heating, Kyoto, Japan, 1986 (unpublished).

[11]J. Y. Hsu and M. S. Chu, Phys. Fluids **30**, 1221 (1987).

[12]C. M. Bishop, Nucl. Fusion **26**, 1063 (1986).

[13]J. Gernhardt *et al.*, Max-Planck-Institut für Plasmaphysik Report No. III/59, 1980 (unpublished).

[14]O. Klüber *et al.*, in *Proceedings of the Thirteenth European Conference on Controlled Fusion and Plasma Heating, Schliersee, West Germany,* edited by G. Briffod and M. Kaufmann (European Physical Society, Petit-Lancy, Switzerland, 1986), p. 136.

[15]J. A. Holmes *et al.*, Phys. Fluids **25**, 800 (1982).

[16]N. T. Gladd *et al.*, Phys. Fluids **23**, 1182 (1980).

[17]B. Carreras *et al.*, Phys. Rev. Lett. **50**, 503 (1983).

[18]J. Manickam *et al.*, Nucl. Fusion **27**, 1461 (1987).

[19]T. S. Hahm and P. H. Diamond, Phys. Fluids **30**, 133 (1987).

[20]C. Z. Cheng *et al.*, Plasma Phys. **29**, 351 (1987).

[21]J. A. Wesson, Nucl. Fusion **18**, 87 (1978).

[22]G. v. Gierke *et al.*, in *Proceedings of the Twelfth European Conference on Controlled Fusion and Plasma Physics, Budapest, Hungary, September 1985,* edited by L. Pocs and A. Montvai (European Physical Society, Petit-Lancy, Switzerland, 1985), p. 331.